Solitary Waves and Fluctuations in Fragile Matter

Upadhyaya, N.

Cover Page

Universiteit Leiden

The handle http://hdl.handle.net/1887/22138 holds various files of this Leiden University dissertation.

Author: Upadhyaya, Nitin
Title: Solitary waves and fluctuations in fragile matter
Issue Date: 2013-11-05

INTRODUCTION

Materials are conventionally classified in one of three states of matter: solid, liquid or gas. However, many commonly available materials may be easily arranged to display novel properties, that defy their simple classification into any of the above states of matter. Consider for instance, a block of steel, see Fig . (1.1). It is clearly a solid – if we hammer one end gently, the material remains intact and we hear sound. Now, construct out of the block of steel many smaller steel balls and pack them together so that the balls just touch each other. What happens if we now hit one end of this packing ?

No matter how gently you touch the sample, super-sonic waves (waves that travel faster than the sound speed of the medium) , rather than ordinary sound, will propagate in the packing. This happens no matter how hard (or soft) the constituent balls are. Surprisingly then, this simple aggregate of steel balls already uncovers a unique state of matter, that we will call *fragile matter*.

What is the origin of such an extreme response ? The paradigm of solids is the long range ordering of identical constituents (such as atoms) that interact harmonically for small displacements from their equilibrium lattice spacing. Within such approximations, their response to any external mechanical perturbation is linear and is embodied in a finite elastic moduli that also endows the solid with a finite speed of sound. Higher order non-linear terms conventionally appear as small perturbations around a response that is predominantly linear.

By contrast, in the above example of a granular aggregate of steel balls just in contact with their nearest neighbours, both the linear elastic moduli and speed of sound drop to zero. This extreme *softness* stems directly from the local strongly *non-linear* interaction between macroscopic balls in contact since the interparticle interaction now no longer has a harmonic part. Moreover, this behaviour is independent of the material the ball is made of which could be as hard as steel or as soft as bubbles - it is a result of continuum elasticity that dictates the nature of the interaction between macroscopic objects in contact [1]. This is just one example of how *fragility* originates. Note, the

In fragile matter near their critical point, energy propagates through strongly non-linear waves that travel faster than the speed of sound

notion of a granular aggregate of steel balls as constituting a state of matter, is now at one higher level of abstraction: we are considering the collective behaviour of an aggregate of macroscopically solid balls and studying its mechanical (collective) response.

Interestingly, fragility itself can also arise from a global criteria, for instance in a weakly connected network of cross-linked polymers that are often modelled as a random network of harmonic springs. Here, *softness* in linear response can arise irrespective of the strength of the local spring constant, provided that the number of mechanical constraints is too low to maintain rigidity. In these physical systems, the disordered arrangement of particles plays a pivotal role in shaping the mechanical response by causing the particle displacement field in response to strains applied at the boundaries, to be very heterogeneous (not mimic the direction of strains applied at the boundaries). Such displacements are called *non-affine* and by absorbing a substantial part of the energy supplied at the boundaries, these displacements allow new configurations to minimize the energy, causing a vanishingly small linear response[2, 3, 4].

In many materials (see Fig. (1.2)), it is often the interplay between the nature of the constituents (that dictates their interaction locally) and how they are arranged in the material (global criteria), that together determine the nature of the elastic response. Note here, the notions of *fragility* and *softness* are only to stress the unusual behaviour within the regime of linear response and does not necessarily imply a breaking apart of the material.

In the following sections, we now give some examples of the kinds of unusual behaviour that arise in simple (often idealized) model systems, that are used to study fragile states of matter.

Fragility can arise from local non-linear interactions and/or emerge as a collective phenomenon where disorder plays a pivotal role.

1.1 STRONGLY NON-LINEAR WAVES IN FRAGILE MATTER

1.1.1 *Hertz interaction for elastic bodies*

As alluded to above, the strongly non-linear interaction potential between macroscopic bodies in contact is often a source of fragility. Here, we provide a simple intuitive explanation of the origins of a strongly non-linear elastic response. Detailed analytic derivation may be found in Lev Landau's book on the Theory of Elasticity [5].
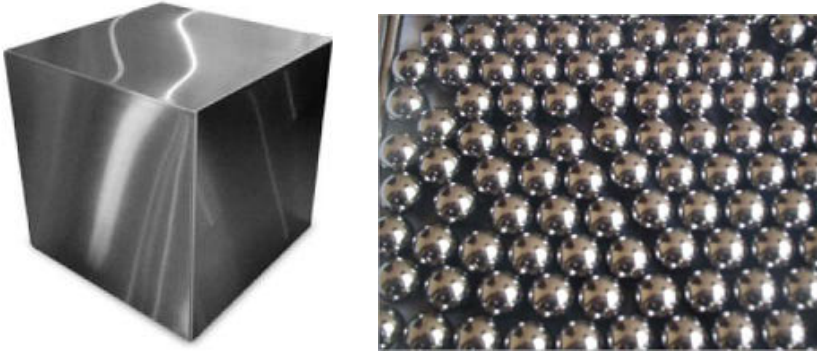
Figure 1.1: A block of steel (left) has a finite speed of sound (6000 m-sec). However, if we cut the block of steel into smaller steel balls and arrange the balls such that they are just touching each other, we uncover a new mechanical state where the sound speed is zero. Energy propagation therefore happens through strongly non-linear waves. This extreme response follows from the non-linear inter-particle interaction and motivates calling this new state as *fragile matter*. Source for figures: *google*.

When two macroscopic objects are brought into contact an elastic deformation δ is generated, as illustrated in Fig. 1.3 [1]. If a ball of radius R is squeezed against a flat wall, it is compressed in the longitudinal direction and expands in the transverse direction. Simple geometric considerations reveal that the radius of the area of contact is approximately $(R\delta)^{\frac{1}{2}}$ (see Fig. 1.3). Therefore in the contact area, the deformation (or strain) γ can be estimated by dividing the longitudinal deformation δ by this radius: $\gamma = \frac{\delta}{(R\delta)^{\frac{1}{2}}} \sim \delta^{\frac{1}{2}}$. According to linear elasticity, for small strains, the stress σ is proportional to the strain γ so that $\sigma \sim \delta^{\frac{1}{2}}$. The corresponding force f is obtained by multiplying the stress by the area of contact, which is proportional to $R\delta$, see the dashed circle in the Figure. The Hertzian law of interaction then follows: $f \sim \delta^{\frac{3}{2}}$, where only the dependence on δ has been kept explicitly. Note that, despite the linear stress-strain relation for the balls material, their interaction force is non-linear.

1.1.2 *A prelude to non-linear waves*

Consider now a general oscillator of the form described above with a return force given by $f \sim \delta^{\alpha-1}$, where δ is the displace-

Figure 1.2: Real examples of fragile matter: (left) a polymer like network of biological muscle fibres , (center) an amorphous packing of tennis balls and (right) bubbles. Source for figures : *google.*

ment from the equilibrium position and $\alpha >= 2$. In the absence of any dissipation, the total mechanical energy is conserved and is the sum of kinetic and potential energies:

$$E = \frac{1}{2}\left(\frac{d\delta}{dt}\right)^2 + \delta^{\alpha}. \tag{1.1}$$

Since E is a constant, we obtain a differential equation for the variable δ,

$$\left(\frac{d\delta}{dt}\right) = \sqrt{2(E - \delta^{\alpha})}, \tag{1.2}$$

solving which, we obtain the time period of oscillation

$$T = \sqrt{2}\int_{-A}^{A}\frac{d\delta}{A^{\alpha} - \delta^{\alpha}}, \tag{1.3}$$

where, we have defined the amplitude of oscillation $A = E^{\frac{1}{\alpha}}$. Defining a new variable $t = \left(\frac{\delta}{A}\right)^{\alpha}$, the integral can be simplified and expressed in the form a Beta integral

$$T = \frac{2\sqrt{2}}{A^{\frac{\alpha-2}{2}}}\int_0^1 dt \; t^{\frac{1}{\alpha-1}}(1 - t)^{-\frac{1}{2}} \tag{1.4}$$

with the solution

$$T = \frac{2\sqrt{2}}{A^{\frac{\alpha-2}{2}}}\frac{\Gamma\left(\frac{1}{2}\right)\Gamma\left(\frac{1}{\alpha}\right)}{\Gamma\left(\frac{1}{2} + \frac{1}{\alpha}\right)}. \tag{1.5}$$

Notice now, the time period or equivalently, the frequency of oscillation depends upon the amplitude as $\omega \sim A^{\frac{\alpha-2}{2}}$ for $\alpha > 2$ (non-linear oscillator) but is independent of the amplitude for $\alpha = 2$ (harmonic oscillator).
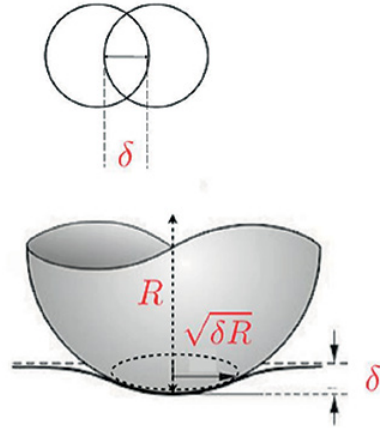
Figure 1.3: Schematic illustation of the origin of non-linear Hertz law of interaction between macroscopically large bodies interacting elastically. The top inset shows two sphere with an overlap δ. In the bottom figure, a sphere is pressing against a flat surface that causes both compression by an amount δ and lateral deformation proportional to $\delta^{\frac{1}{2}}$. *source : Shocks in fragile matter [1]*

This dependence of the frequency of oscillation upon the initial condition or the amplitude of excursion is the crucial difference between a harmonic oscillator with a linear restoring force (simply called a linear oscillator, such as the simple pendulum) and a non-linear oscillator and already alludes to the notion of non-linear waves. Recall, a linear non-dispersive wave typically assumes the form $\psi(x, t) = AG(x - ct)$, where A is the amplitude, $c = \omega/k$ is the constant speed of sound that only depends on the material properties of the medium, k is the wave-number and ψ, G are some general functions. Roughly then, since for a non-linear wave the frequency of oscillation is a function of the amplitude $\omega \equiv \omega(A)$, therefore the speed of propagation also depends upon the amplitude of the wave $c(A)$. In subsequent sections, we will explore specific examples where the dependence of the speed of propagation of the wave on its amplitude will signal the onset of a non-linear regime.

1.1.3 *Examples of fragile matter in one dimension*

One of the simplest example of fragile matter is a one dimensional chain of spherical macroscopic beads that are just in contact with their two nearest neighbours. Since this is a perfectly

ordered arrangement, we could try to define an effective spring constant from the second derivative of the interaction potential. Consider an interaction potential of the generalized Hertz form, i.e., $V(\delta) \sim \delta^\alpha$, where $\alpha > 2$ is the non-linear exponent. The case $\alpha = \frac{5}{2}$ corresponds to the Hertz law of interaction for linear macroscopic objects as described in section 1.1.1.

Using the second derivative of the potential to define an effective spring constant, we find, $K_{eff} \sim \delta^{\alpha-2}$. For a vanishingly small initial overlap, $\delta \equiv \delta_0 \to 0$, and we see that for $\alpha > 2$, $K_{eff} \to 0$, while for $\alpha = 2$, it is a finite constant. Since the speed of sound is related to the effective spring constant as $c \sim \sqrt{K_{eff}}$, we find that in a system that is initially un-stressed $\delta_0 \to 0$ (and has an interaction potential that has no harmonic part), the speed of sound in the medium is zero. Such a unique mechanical state, characterized by the absence of any sound, is referred to as *sonic vacuum*[6].

Consequently, mechanical strains that arise for instance, in response to an impulse given to one of the beads, evolve into strongly non-linear waves that propagate as spatially compact excitations known as solitary waves. Note, in this example we have considered a chain of macroscopic beads (or balls) arranged in a line. In principle, this allows the possibility for the beads to break contact with each other. However, the state of sonic vacuum defined above simply stems from the non-linear power law interaction potential and exists even if we replace the beads with point nodes that interact with a non-linear spring, where both spring stretching and compression are accommodated. In subsequent sections, we will explore these examples in more detail.

1.1.4 *Examples of fragile matter in two dimensions*

As a minimal two dimensional model for fragile matter with disorder, we consider an amorphous packing of frictionless spheres (or disks) that interact repulsively upon overlap (including the possibility of no overlap as in hard disks). The unique control parameter specifying such a system is the packing fraction, ϕ defined as the ratio of the volume occupied by the spheres to the total volume of the sample. Extensive simulations have revealed the existence of a critical packing fraction ϕ_c, at which the packing undergoes a jamming (or rigidity) transition - below ϕ_c, the particles do not overlap and the energy, pressure and number of contacts between particles is zero. Above, ϕ_c

the energy, pressure, number of contacts, shear and bulk modulii are non-zero and scale with the distance from the critical point; $\delta\phi = \phi - \phi_c$.

If the interaction potential between particles that overlap by an amount δ is $V(\delta) \sim \delta^\alpha$, then for $\alpha = 2$ (harmonic interaction), the bulk modulus at the critical point is finite, but it is found that the shear modulus still vanishes. This is an example where fragility arises macroscopically and here, the amorphous arrangement of the spheres plays a crucial role. For $\alpha > 2$ (strongly non-linear interaction), the local spring constant defined as the second derivative of the interaction potential (as in the one dimensional example) vanishes in the limit $\delta_0 \to 0$. Consequently, at the critical point both the bulk and shear modulus are zero.

Another extensively studied model for fragile systems is a random network of harmonic springs that may be derived from the amorphous packing of spheres by replacing their centres with nodes and by modelling the interaction between neighbouring overlapping spheres with springs that can both, stretch and compress (two sided interaction). Such a random network of springs is often also used as a starting point to model polymer networks and glasses. Here, the control parameter is the average number of nodes each node is connected to, i.e., z. If we start with a loose arrangement of spheres, then at the rigidity transition, ϕ_c, the average connectivity z also jumps discontinuously from zero to a critical value $z_c = 2d$ (also called the isostatic value z_{iso}), that according to Maxwell's criteria marks the onset of mechanical rigidity for a lose particulate system in d dimensions. The mechanical properties above the critical value, are seen to scale with the distance from the critical value as $\delta z = z - z_c$.[1]

In these examples, the vanishing of one or both the elastic modulii near the critical point leads to *fragility* that dictates their mechanical properties well beyond the critical point itself. We next explore as a consequence, some of the non-linear excitations that result when we strain at a uniform rate, one of the boundaries of the above model systems.

---

[1] Once a random network is used as a model under study though, there is no constraint in making $z < z_{iso}$ (due to springs that connect neighbouring nodes, it is no longer a loose arrangement of particles) and the mechanical properties below the isostatic value constitutes an active area of research.
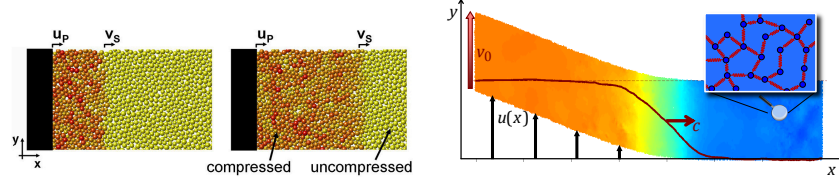
Figure 1.4: Schematic illustration of *left*: compressing an amorphous packing of soft frictionless disks close to the critical packing fraction ϕ_c with a piston moving at a uniform speed u_p. This results in a velocity field (illustrated in red) that corresponds to a uni-axial shock front that propagates along the direction of compression ($x-$direction) at a speed $v_s \sim u_p^{\frac{\alpha-2}{\alpha}}$. *right*: shearing a random network of harmonic springs close to the isostatic value z_c results in a shear front that propagates transverse to the direction of shearing . The velocity field is defined by averaging the longitudinal speeds of nodes. For high strain rates, the speed of propagation of non-linear shear fronts depends upon the applied strain rate as $v_f \sim \gamma^{1/2}$.

1.1.4.1 *Compression shocks in amorphous packings:*

Consider first the two dimensional packing of soft frictionless disks close to the critical point ϕ_c (see Fig. (1.4) left panel), where overlapping nearest neighbours interact with a purely non-linear potential of the form $V(\delta) \sim \delta^\alpha$, $\alpha > 2$. As shown in Fig. (1.4) left panel, compressing one end of the packing at a uniform rate u_p results in a compressive shock front (red field) that propagates along the direction of compression at a speed $v_s \sim u_p^{\frac{\alpha-2}{\alpha}}$ (see Fig. (1.5)). Since on either side of the shock front the number of disks is conserved, the relation between the driving speed u_p and the front speed v_s may be obtained from the conservation of number density.

In a frame of reference moving at the front speed v_s, the flux q to the left of the front equals the flux to its right- $q_l = \rho_l(u_p - v_s) = \rho_r(0 - v_s) = q_r$. This is known as the Rankine-Hugoniot condition for the shock speed:

$$v_s = u_p \frac{\rho_l}{\rho_l - \rho_r}. \tag{1.6}$$

Assuming now, that the average overlap between disks in the un-compressed region (right of the front) is δ_0 and in the compressed region (left of the front) is δ_s, the respective number densities in the two regions are $\rho_l = \frac{1}{2R-\delta_s}$ and $\rho_r = \frac{1}{2R-\delta_0}$,

where R is the average radii of the disks. Substituting in Eq. (1.6), we arrive at $v_s = u_p \frac{2R-\delta_0}{\delta_s-\delta_0}$ which for strongly non-linear fronts $\delta_s \gg \delta_0$, yields $v_s \sim \frac{u_p}{\delta_s}$.

Next, we make the working assumption that the particles enveloped within the region of the shock (see Fig. (1.4) red region) satisfy a Virial-like relation, i.e., in steady state, there exists a balance between the disk kinetic energies and the induced potential energy $u_p^2 \sim \delta_s^\alpha$. Then, the average compression induced by the propagating front is $\delta_s \sim u_p^{\frac{2}{\alpha}}$. This non-trivial scaling relation is a consequence of the non-linear local interactions and is verified numerically[26]. Thus, for strongly non-linear shocks, the shock speed is related to the driving rate via

$$v_s \sim \frac{u_p}{\delta_s} = u_p^{\frac{\alpha-2}{\alpha}}. \tag{1.7}$$

As alluded to earlier, this is a defining feature of non-linear waves: the speed of propagation depends upon the amplitude of the wave, unlike for linear sound waves, where the speed of propagation is independent of the amplitude (for instance, if $\alpha = 2$, v_s becomes independent of u_p). As shown in Fig. (1.5) left panel, this scaling relation is in very good agreement with numerical findings (shown for $\alpha = \frac{5}{2}$) and is also confirmed in recent experiments [7].

1.1.4.2 *Densification fronts in hard sphere gas below the critical point:*

In a recent experimental study, it is shown that uni-axially compressing a two dimensional loose assembly of hard binary disks below the jamming critical density ϕ_j, leads to a densification front that travels along the direction of compression, leaving the region enveloped by the front jammed at ϕ_j [8]. This is analogous to the red region shown in Fig. (1.4) left panel, except that for hard disks, the maximum packing fraction saturates at $\phi_j < \phi_c$. Since the number of disks behind and ahead of the front is conserved, the Rankine-Hugoniot condition Eq. (1.6) still holds. However, for hard disks, the region to the left of the front can be compressed to its maximum density ϕ_j and thus the front speed is simply related linearly to the driving speed $v_s = u_p \frac{\phi_j}{\phi_j-\phi_0}$, where $\phi_0 < \phi_j$ is the initial packing fraction. Notice, this relation is also obtained by taking the hard sphere limit of Eq. (1.7) : $v_s \sim \lim_{\alpha\to\infty} u_p^{\frac{\alpha-2}{\alpha}} = u_p$.

1.1.4.3 *Shear fronts in random spring networks:*

Next, we consider a random network of nodes connected by harmonic springs in the vicinity of the critical point , with an average connectivity $z > z_c$. Here, fragility manifests in the vanishingly small shear modulus that scales linearly with the distance from the critical point $G \sim \Delta z$. Consequently, as we approach the critical point from above, the transverse speed of sound $c \sim \sqrt{G}$ also drops to zero.

This limited window of linear response near the critical point, manifests in a non-linear constitutive stress-strain relation (in the frequency independent regime) for the shear stress as a function of shear strain applied at the boundary: [2]-

$$\sigma = G\gamma + \kappa\gamma|\gamma|. \tag{1.8}$$

Here, $\sigma \equiv \sigma_{xy}$ is the coarse grained shear stress, γ is the shear strain and κ is the coefficient of the first non-linear term (independent of Δz). Upon comparing the two terms on the right hand side, we find the critical strain $\gamma_c = \frac{G}{\kappa}$, beyond which the elastic response is predominantly non-linear. Note that, as we approach the critical point, $\Delta z \to 0$, the critical strain $\gamma_c \to 0$ and thus, an infinitesimally small strain elicits a strongly non-linear response. Since the constitutive random spring network is composed of purely harmonic springs, the strongly non-linear response near the critical point, highlights the macroscopic fragility of these networks, although the origins of non-linearity remain local (see Supplementary Information E).

The dynamics of energy propagation can now be explored by conducting numerical experiments analogous to the ones considered previously for an amorphous packings of frictionless spheres, but now in the transverse direction. Here, it is found that by shearing one edge of the sample at a uniform rate below the critical strain rate $\dot{\gamma}_c$ (in dimensionless units, the strain and strain rates coincide), initially gives rise to a transient super-diffusive spreading of the transverse velocity field away from the shearing zone, see Fig. (1.4) right panel. At later times however, this crosses over into a well defined shear front that propagates with the transverse speed of sound $c \propto \sqrt{G}$. Interestingly though, the linear shear fronts are not in a steady state, i.e., their widths continue to increase with time. We understand this behaviour as arising from the increasingly heterogeneous elastic displacement field near the critical point, that makes the random spring networks an over-damped system, despite no microscopic mechanism for dissipation being present. This unique

feature is a direct evidence of how the underlying network disorder manifests in the properties of the shear front, causing their widths to spread diffusively with time [9].

For strain rates $\gamma > \gamma_c$, the constitutive stress-strain relation described by Eq. (1.8) is non-linear and results in supersonic shear fronts. From Eq. (1.8), we identify a *non-linear modulus* $G_{nl} = G + \kappa\gamma$, and consequently a characteristic non-linear speed of propagation that is a function of the applied strain rate:

$$v_f = \sqrt{\frac{G_{nl}}{\rho}} = \sqrt{c^2 + \frac{\kappa\gamma}{\rho}} \ . \tag{1.9}$$

Notice, for $\gamma \ll \gamma_c$, the front speed approaches the transverse speed of sound c and is independent of the strain rate (driving amplitude). On the other hand, for $\gamma \gg \gamma_c$, the front speed becomes independent of c (and hence Δz), and depends only upon the applied strain as $v_f \propto \gamma^{\frac{1}{2}}$, this we classify as the strongly non-linear regime.

In Fig. (1.5) , right panel, we see the analytically predicted speed of propagation Eq. (1.9)(solid lines) compared against numerical findings (symbols) for a range of dz. For $\gamma < \gamma_c$, the speed of propagation is independent of the applied strain rate and agrees very well with the numerically determined transverse speed of sound. For $\gamma > \gamma_c$, we observe non-linear fronts that propagate at speeds that depends on the applied strain rate and the numerical findings are in very good agreement with the analytical estimate in Eq. (1.9). For $\gamma \gg \gamma_c$, we enter a strongly non-linear regime where the front speed depends quadratically upon the applied strain rate as $v_f \propto \gamma^{\frac{1}{2}}$ while becoming independent of Δz.

The behaviour of shear fronts in the strongly non-linear regime is analogous to the strongly non-linear compressional fronts observed in amorphous packings of soft frictionless disks where for sufficiently large driving speeds, $v_s \sim u_p^{\frac{1}{5}}$ (for $\alpha = \frac{5}{2}$ independent of the packing fraction). Thus, we find that despite the disparate sources of fragility (local versus global), the physics of energy propagation in the form of strongly non-linear waves is one of the defining features of fragile matter near their critical point. Note also, despite the differing exponents that capture the front speed as a function of driving rate, in both cases, the front speeds in the strongly non-linear regime is independent of the underlying microstructure, not being dependent on the distance from the critical point ($\delta\phi$ or δz).
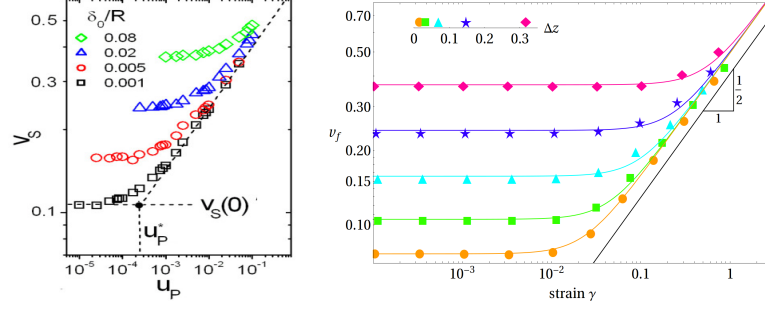
Figure 1.5: The front speed as a function of applied strain rate for
left: compressional shocks in a jammed amorphous pack-
ing of soft frictionless disks for $\alpha = \frac{5}{2}$ in agreement with
the relation $v_s \sim u_p^{\frac{1}{5}}$ (dashed line) for high strain rates.
The symbols correspond to numerical data of the front
speed, obtained for a range of initial packing fractions
δ_0. *right*: shear fronts in random network of harmonic
springs shown for a range of coordination numbers dz.
The solid lines correspond to the analytical prediction Eq.
(1.9) while symbols correspond to numerical data for the
front speed.

1.2 DISORDER AS AN EFFECTIVE VISCOSITY ?

Understanding the nature of disorder in amorphous materials
is still an arduous task. In particular, for fragile matter near the
critical point, the breakdown of linear elasticity and the result-
ing non-linear response makes a quantitative analysis difficult.
Notwithstanding, disorder has some clear signatures in the dy-
namical response of these systems, that we could try to explore.

At a simpler, qualitative level, the process of defining uni-
axially propagating fronts involves an averaging over the de-
grees of motion transverse to the direction of propagation. See
for instance Fig. (1.4), where for compressional fronts propagat-
ing along the horizontal $x-$ direction, an averaging of the par-
ticle speeds over the transverse y- direction is necessary. Simi-
larly for the shear fronts, an averaging along the horizontal di-
rection is implied. For amorphous packings, this process thus
necessarily involves ignoring a part of the energy that is being
supplied at the boundaries. The net result is that this loss of en-
ergy effectively acts as a source of dissipation, that we refer to
as an effective viscosity. The way this effective viscosity mani-
fests in the properties of the propagating fronts however, differs
in details.

The steadily propagating compressional shocks in amorphous packings are a consequence of the interplay between locally non-linear inter-particle interaction potential and the granular nature of the medium, that acts as a source of dispersion. The shock widths are thus a few grain diameters and happen to be, independent of the shock amplitude. As a result, the leakage of energy (or the effective viscosity) into degrees of motion transverse to the direction of propagation of the front, do not effect the shock width but act as a small perturbation that smooths out the shape of the shock profiles, in contrast to the oscillatory profiles observed in more ordered packings [26]. [2]

By contrast, both the linear and non-linear shear fronts observed in random spring networks are a macroscopic phenomenon. The increasingly heterogeneous (non-affine) elastic displacement field close to the isostatic value, spills a large part of the energy into degrees of motion transverse to the ones being excited at the boundaries. For shear fronts, this amounts to a loss of energy into longitudinal excitations and several numerical studies have indicated that this loss diverges with the distance from the critical point $l^* \sim \Delta z^{-1/2}$. Consequently, both in the linear and non-linear regimes, random spring networks are found to be over-damped and the propagating fronts never achieve a steady state. Instead, their widths continue to grow with time. For instance, upon rescaling the temporal diffusive spreading of the linear shear fronts for strain rates $\gamma < \gamma_c$, the front widths are observed to be dictated by the diverging length l^*. Since this effect mimics the effect of viscosity (in setting the width of the shock transition region), disorder emerges as an effective viscosity that diverges as the critical point [9].

The densification fronts observed below the hard disk jamming density ϕ_j are found to be in a steady state and satisfy a Burgers-like non-linear diffusion equation. Like the shear fronts in random spring networks, a diverging length scale $l_j \sim (\phi_j - \phi_0)^{-0.65}$ sets the widths of the propagating fronts that now scales as $\eta = u_p l_j$, where u_p is the driving speed [8]. Physically, the length scale l_j here is found to be the characteristic length scale associated with longitudinal velocity-velocity correlation function.

---

[2] It is not the intention to convey here that these observations are obvious. We are only drawing some of these conclusions after having done the numerical experiments.

1.3   THIS THESIS

As part of this thesis, we will try to understand the interplay between the strongly non-linear waves and the underlying disorder, in models of fragile matter that are in the vicinity of the critical point. For instance, to better understand the role of disorder in jammed amorphous packings close to their critical packing fraction, we will study what happens to an impulse that is imparted at one of the edges of such a packing. This is in contrast to the compression experiments discussed previously, where an amorphous packing of soft frictionless disks is compressed at a uniform rate resulting in steadily propagating shock fronts. Rather, the study of impulse propagation will somewhat simplify the analysis and bring to the fore, the role played by disorder as a mechanism that continually takes energy away from the propagating excitation.

As our first step towards this, we will consider a two dimensional hexagonal packing of soft frictionless disks that are just in contact with their nearest neighbours and thereby, constitute a state of sonic vacuum (upon overlap the disks interact with the nonlinear Hertz potential). As the simplest form of disorder, we will consider an isolated impurity that we model as an interface that separates two hexagonal packings composed of disks with different masses so that on one side of the interface all the disks (particles) have a mass m_1 and on the other side all the disks have a mass m_2. The elastic isotropy of the hexagonal lattice will essentially reduce the study of impulse propagation to a one dimensional problem, whose analytic solitary wave solutions are by now well established. Consequently, by mapping the resulting solitary wave excitation to a quasi-particle with an effective mass, we will be able to (approximately) understand the interaction of the solitary wave with the interface for different choices of mass ratios $A = m_2/m_1$.

Our understanding of the solitary wave behaviour across the interface will equip us with some approximate analytical tools to then study the problem of solitary wave propagation in a hexagonal lattice with particle masses distributed randomly. Subsequently, we will find a good estimate of how increasing the disorder (variance in mass distribution), increases the damping rate of the propagating solitary wave.

For a larger variance in the mass distribution, we will find a new regime of wave propagation and an associated decay rate. We will see that it is no longer possible to identify a propagat-

ing solitary wave except at the very early stages of the evolution of the impulse. Instead, we will find that the initial impulse soon transitions into a triangular shock like propagating front whose amplitude decays as it traverses the medium. This extreme limit of high disorder in particle masses then provides us with a link to the physics of impulse attenuation in amorphous packings where again an initial impulse transitions into a triangular shock front whose amplitude decays with the same power law exponent as in the hexagonal packing.

The attenuation of the impulse then leads to some interesting consequences. As noted, disorder will cause the energy initially localized in an impulse to be distributed throughout the amorphous packing (of finite size). Consequently, in a system with no intrinsic mechanism to dissipate energy, the particles will continue to fluctuate forever. This we imagine as a granular analogue of temperature where the passage of the impulse effectively fluidizes the amorphous packing and where the energy of the impulse plays a role that is analogous to temperature (but not really in thermal equilibrium). As a consequence, the emergent mechanical state will have a finite bulk modulus and a viscosity that we will see is consistent with the description of a one dimensional fluid in equilibrium (recall, we started with an amorphous packing at the critical point where it has vanishingly small bulk and shear modulus).

The emergence of a granular analogue of temperature and a fluctuation induced rigidity then motivates us to study an example of fragile matter that is explicitly coupled to a source of thermal fluctuation. The coupling to the heat bath forces the system to be truly in a state of thermal equilibrium. As the simplest toy model, we will adopt a one dimensional chain of strongly non-linear Hertz springs coupled to a heat bath. We will then study the propagation of an impulse along this chain and find that for small thermal fluctuations, the impulse again evolves into the same solitary wave solution that are the characteristic excitations in a granular chain of beads. By mapping the solitary wave to a quasi-particle, we will find that its dynamics can be described in analogy with that of a Brownian particle.

In the last chapter, we will shift our attention to another model of fragile matter: a two dimensional disordered network of linear springs, where the loss of rigidity (vanishing shear modulus) is a collective phenomenon. By shearing one edge of the sample at a uniform rate we will study the resulting dynamics, finding both a linear and non-linear regime for the propa-

gation of the shear front. In addition, within the linear regime, we will find that at early times, there is no front propagation but only a super-diffusive spreading of the energy away from the shearing edge.

GRANULAR INTERFACES

In order to build up the tools to study the propagation of strongly non-linear solitary waves in a two dimensional amorphous material, we begin here by looking at the interaction of the solitary wave with an isolated impurity modelled as a granular interface formed between two hexagonal lattices comprising particles with different masses. By treating the solitary wave as a quasi-particle with an effective mass, we construct an intuitive (energy and linear momentum conserving) discrete model to predict the amplitudes of the transmitted and reflected solitary waves generated when an incident solitary wave, parallel to the interface, moves from a lighter/denser to a denser/lighter granular hexagonal lattice [‡].